Langmuir

Letter

pubs.acs.org/Langmuir

Synthetic Mimics of Bacterial Lipid A Trigger Optical Transitions in Liquid Crystal Microdroplets at Ultralow Picogram-per-Milliliter Concentrations

Matthew C. D. Carter,[†,§] Daniel S. Miller,[‡,§] James Jennings,[†] Xiaoguang Wang,[‡] Mahesh K. Mahanthappa,[*,†,‡,∥] Nicholas L. Abbott,[*,‡] and David M. Lynn[*,†,‡]

[†]Department of Chemistry, and [‡]Department of Chemical and Biological Engineering, University of Wisconsin—Madison, Madison, Wisconsin 53706, United States

Supporting Information

ABSTRACT: We report synthetic six-tailed mimics of the bacterial glycolipid Lipid A that trigger changes in the internal ordering of water-dispersed liquid crystal (LC) microdroplets at ultralow (picogram-per-milliliter) concentrations. These molecules represent the first class of synthetic amphiphiles to mimic the ability of Lipid A and bacterial endotoxins to trigger optical responses in LC droplets at these ultralow concentrations. This behavior stands in contrast to all previously reported synthetic surfactants and lipids, which require near-complete monolayer coverage at the LC droplet surface to trigger ordering transitions. Surface-pressure measurements and SAXS experiments reveal these six-tailed synthetic amphiphiles to mimic key aspects of the self-assembly of Lipid A at aqueous interfaces and in solution. These and other results suggest that these amphiphiles trigger orientational transitions at ultralow concentrations through a unique mechanism that is similar to that of Lipid A and involves formation of inverted self-associated nanostructures at topological defects in the LC droplets.

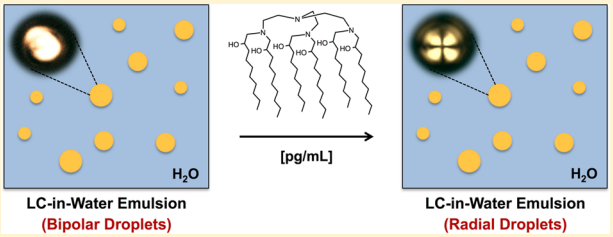

INTRODUCTION

Materials that exhibit macroscopic and easily transduced changes in properties in response to specific molecular stimuli offer unique opportunities to design new classes of sensors and actuators. In this context, supramolecular materials—which derive their structures and properties from weak, noncovalent interactions—are particularly promising because the ordering of these assemblies is easily perturbed by molecular interactions, and the dynamics of reorganization induced by stimuli can be fast.[1−5] In particular, recent studies have demonstrated that a variety of molecular species and assemblies—ranging from simple synthetic surfactants to polyelectrolyte assemblies and protein-receptor complexes—can trigger ordering transitions in thin films and water-dispersed microdroplets of thermotropic liquid crystals (LCs) in ways that can be readily observed and quantified using light.[6−17] These ordering transitions are sensitive to even very small changes in the structures or concentrations of environmental analytes, and thus provide a basis for the design of exceedingly sensitive LC-based sensors.

Of particular relevance to the work reported here, we recently reported that bacterial endotoxins and their six-tailed glycolipid component Lipid A (Figure 1A) can trigger ordering transitions in micrometer-size droplets of LC at remarkably low concentrations (e.g., 1 pg/mL in water; from the so-called "bipolar" to the "radial" state, see Figure 1D−I and additional discussion below).[9,18] In contrast, all one- and two-tailed synthetic surfactants and other biological lipids investigated to date trigger ordering transitions in the 10−100 μg/mL range—concentrations that lead to near-complete monolayer coverage of the LC droplets and are 5−6 orders of magnitude *higher* than those at which Lipid A elicits a response.[8,9,18] The results of past studies suggest that Lipid A promotes optical transitions in LC droplets at such ultralow concentrations through a fundamentally new mechanism that involves the formation of inverted self-associated nanostructures at topological defects in the LC.[9,18] The study reported here was motivated by the goal of providing insight into the origins of this ultrasensitive and specific response of LC microdroplets to Lipid A by exploring designs of synthetic amphiphiles (e.g., Figure 1B) inspired by salient structural features of Lipid A.[19,20]

The design of the synthetic amphiphiles reported here was guided by the hypothesis that the sensitivity of LC droplets to Lipid A arises principally from the multiplicity of tails present in this natural lipid. The six tails of Lipid A, for example, render it more hydrophobic than one- and two-tailed amphiphiles and endow it with other properties (e.g., negative spontaneous curvature resulting from a large ratio of tail volume to headgroup area) that promote the formation of inverted self-associated structures.[21,22] We note that past studies have

Received: September 24, 2015
Revised: November 11, 2015
Published: November 12, 2015

DOI: 10.1021/acs.langmuir.5b03557
Langmuir 2015, 31, 12850−12855

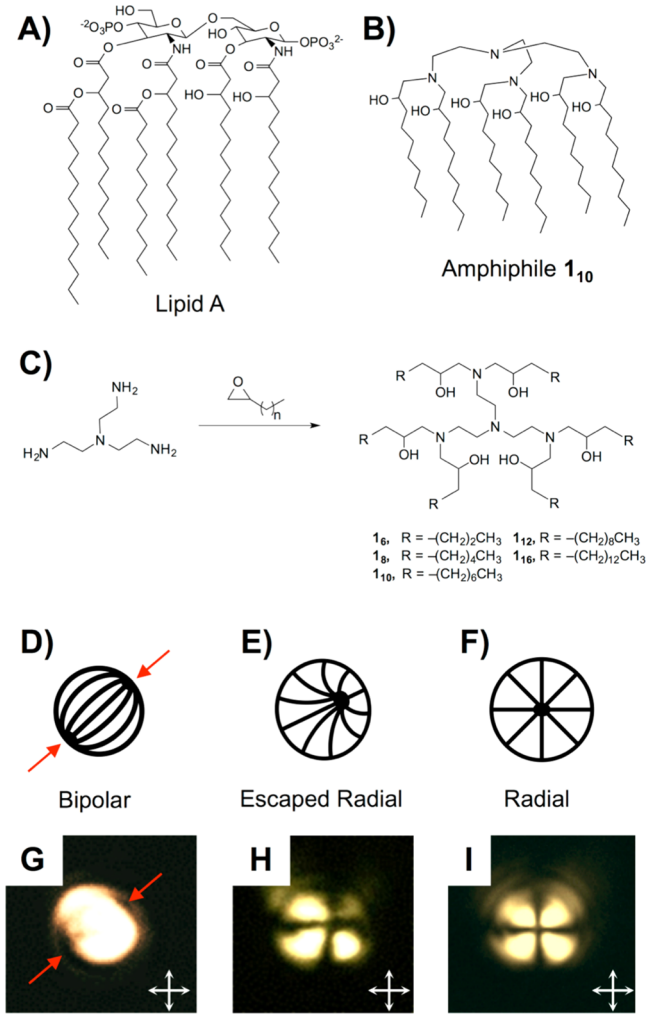

Figure 1. (A,B) Structures of Lipid A and amphiphile $\mathbf{1}_{10}$. (C) Synthesis of six-tailed Lipid A mimics. (D–F) Director profiles for LC droplets in (D) bipolar, (E) escaped radial, and (F) radial configurations. (G–I) Polarized light micrographs of microdroplets of 5CB (diameters of ~5 μm) prior to (G) and after (H and I) exposure to amphiphile $\mathbf{1}_{10}$ (see text). Red arrows in (D) and (G) point to topological defects in the bipolar droplets; white arrows (G–I) indicate orientation of crossed polarizers.

reported structurally complex mimics of Lipid A designed to preserve elements of the function of this amphiphile in biological contexts.[19] In contrast, the work reported here sought to explore the design of simple synthetic amphiphiles that mimic aspects of the structure of Lipid A that govern its behavior at liquid/liquid interfaces and trigger ordering transitions in LC droplets, with the goals of (i) providing insights into molecular mechanisms through which LC microdroplets respond to Lipid A, and (ii) expanding the potential significance of the ultrasensitive response of LC microdroplets to Lipid A by incorporating functionality into synthetic mimics that could enable additional stimuli-responsive properties.

EXPERIMENTAL SECTION

Materials. Tris(2-aminoethyl)amine (TREN) was purchased from Acros Organics. Aliphatic epoxides were purchased from TCI America or Alfa Aesar. Lipid A from *E. coli F583* was purchased from Sigma-Aldrich. The LC 4′-pentyl-4-cyanobiphenyl (5CB) was obtained from EM Sciences. A description of additional materials used is provided in the Supporting Information. Unless otherwise noted, materials were used as received.

Synthesis of Amphiphiles. Amphiphiles $\mathbf{1}_6$–$\mathbf{1}_{16}$ were synthesized using the following general procedure. TREN (1.0 equiv) and an epoxide having the desired aliphatic chain length (6.6 equiv) were purged with nitrogen and heated at 90 °C for 4 days. Reaction products were purified by flash chromatography on silica gel. ^{1}H NMR and ^{13}C NMR spectra for each amphiphile and additional experimental details are included in the Supporting Information.

Preparation and Characterization of LC Emulsions. LC-in-water emulsions were formed by adding 6 μL of 5CB to a glass tube, adding 3 mL of a 10 μM solution of SDS in EndoTrap Red Equilibration Buffer, and vortexing for 30 s at 3000 rpm. Aliquots (70 μL) of these emulsions were diluted into 700 μL of aqueous dispersions of either Lipid A or a synthetic amphiphile, and the emulsion was allowed to sit for at least 3 h before characterization by light scattering (using flow cytometry) or by polarized light microscopy. Frequency histograms of the intensity of forward light scattering (FSC) were obtained for LC emulsions using a BD Accuri C6 flow cytometer. FSC was measured at a detection angle of 0° ± 15°, and histograms were constructed from data collected from the measurement of 5,000 droplets. The percentage of radial droplets was quantified using a previously reported procedure described in greater detail in the Supporting Information.

Small-Angle X-ray Scattering (SAXS). SAXS measurements were performed using a Bruker D8 Discover diffractometer. Amphiphiles were weighed into a glass vial to which 20 mL of 1 M H_2SO_4 was added to give a final amphiphile concentration of 0.133 wt %. Samples were vortexed, sonicated, and transferred to quartz capillaries and sealed. SAXS analysis was performed with Cu Kα X-rays produced from a micro X-ray source with a Montel mirror passed through a 0.5 mm pinhole to collimate the beam. Two-dimensional (2-D) scattering patterns were collected on a VANTEC-500 detector (140 mm in diameter; sample-to-detector distance of 22.26 cm) calibrated with a silver behenate standard (d = 58.38 Å). Additional details related to the integration and fitting of scattering data are included in the Supporting Information.

RESULTS AND DISCUSSION

To design synthetic mimics of Lipid A, we adopted an approach based on the ring-opening of 1,2-epoxyalkanes by primary amines (Figure 1C) for the following reasons: (i) these reactions are robust and proceed in a single step, (ii) this scheme provides ready access to amphiphiles possessing many aliphatic tails, (iii) both headgroup structure and the number, length, and structure of hydrophobic tails can be varied systematically, and (iv) each ring-opening reaction affords a hydroxyl group that can be further transformed, if desired, to modify the structures, properties, and phase behaviors of the resulting amphiphiles. This synthetic approach has been used in recent studies to design cationic lipid-like molecules for nucleic acid delivery,[23−26] but reports on the behaviors of this class of amphiphile in aqueous solution and at aqueous/organic interfaces are limited.

We synthesized five six-tailed amphiphiles with aliphatic tail lengths ranging from 6 to 16 carbons by the reaction of tris(2-aminoethyl)amine with a series of 1,2-epoxyalkanes (amphiphiles $\mathbf{1}_6$–$\mathbf{1}_{16}$; Figure 1C).[23] In the notation used here, the subscript indicates the number of carbons in each aliphatic tail, such that amphiphile $\mathbf{1}_{10}$ consists of a headgroup containing four tertiary amines to which six aliphatic tails, each 10 carbons in length, are bound. All compounds were purified by flash chromatography; structure and purity were confirmed by NMR and mass spectrometry (see the Supporting Information).

In a first set of studies, we characterized the ability of amphiphile $\mathbf{1}_{10}$ to trigger ordering transitions in micrometer-

DOI: 10.1021/acs.langmuir.5b03557
Langmuir 2015, 31, 12850−12855

sized droplets of a nematic LC [4′-pentyl-4-cyanobiphenyl (5CB)] using a protocol reported previously to characterize interactions between Lipid A and bacterial endotoxin in LC-in-water emulsions.[9,18] For these experiments, an aqueous dispersion of LC droplets (~5000 droplets/μL) in a "bipolar" configuration was added to a solution of $\mathbf{1}_{10}$ to achieve a final concentration of 1000 pg/mL (in the "bipolar" configuration, the LC is aligned tangentially to the droplet surface, resulting in two topological defects at opposite poles; see Figure 1D,G).[17] Changes in droplet configurations were then determined using polarized light microscopy (see the Supporting Information for details). An amphiphile concentration of 1000 pg/mL was selected as an upper limit for these studies because it corresponds to a concentration 3 orders of magnitude below that required to trigger ordering transitions in LC droplets using conventional surfactants and lipids.[8,9]

Following the addition of amphiphile $\mathbf{1}_{10}$, we observed all LC droplets to transition from the initial bipolar state (Figure 1D,G) to either a "radial" configuration (in which the director of the LC is aligned normal to the droplet surface, resulting in a single defect at the center of the droplet; Figure 1F,I) or an "escaped radial" configuration (Figure 1E,H).[17] In the escaped radial configuration, a single defect similar to that observed in radial droplets is located near, but not in, the geometric center of a droplet (Figure 1E). This configuration has an optical appearance (Figure 1H) that can also be readily distinguished from that of a bipolar droplet when viewed between crossed polarizers.

We further quantified the response to amphiphile $\mathbf{1}_{10}$ in larger populations of LC droplets using flow cytometry. This analytical approach can be used to quantify the percentage of radial droplets in mixtures containing bipolar and radial droplets based on differences in the scattering of light and is significantly faster than methods based on optical microscopy.[27] We characterized the dependence of changes in LC droplet configurations at 5 different concentrations of amphiphile $\mathbf{1}_{10}$ (ranging from 10 to 10 000 pg/mL). We note here that our analysis of scatter plots obtained using flow cytometry (in light scattering mode) enabled us to differentiate between either (i) bipolar or (ii) radial and escaped radial droplets combined (see the Supporting Information and Figure S1 for details). Accordingly, we report in Figure 2A the percentage of droplets transformed from the bipolar configuration relative to all droplets characterized. This analysis reveals $\mathbf{1}_{10}$ to trigger ordering transitions in droplets of 5CB at concentrations as low as 100 pg/mL, but not at 10 pg/mL (Figure 2A).

Although the threshold concentration required to trigger complete conversion of the bipolar LC droplets using amphiphile $\mathbf{1}_{10}$ is an order of magnitude higher than that of Lipid A, we note that it is 4 orders of magnitude lower than the concentrations at which conventional surfactants trigger these transitions.[9] As noted above, past studies using conventional one- and two-tailed amphiphiles have established that ordering transitions in LC droplets require near-complete monolayer coverage of amphiphiles over the droplet surface.[9] At a concentration of 100 pg/mL, however, we calculate the maximum areal density of $\mathbf{1}_{10}$ at the interface of the LC droplets in the experiments above (assuming complete adsorption onto the ~3.9×10^6 droplets in the dispersion) to be 5000 nm^2/molecule, or only ~10^{-4} of monolayer coverage. Similar to Lipid A, this interfacial concentration of amphiphile $\mathbf{1}_{10}$ is orders of magnitude below that required to trigger changes in the configurations of the LC droplets via

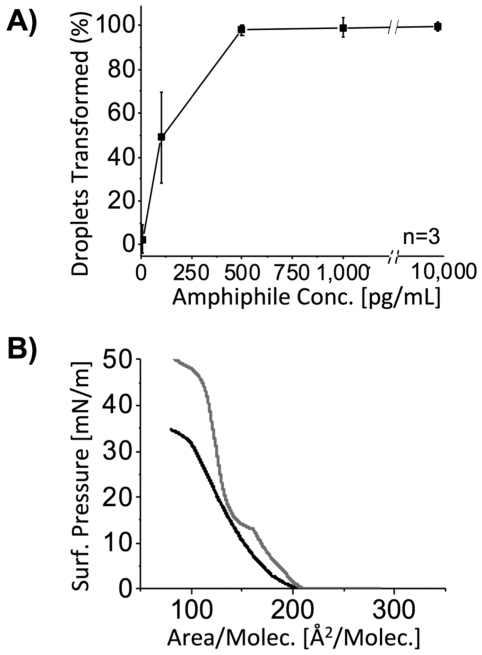

Figure 2. (A) Percentage of droplets transformed from the bipolar state vs concentration of amphiphile $\mathbf{1}_{10}$ as determined using flow cytometry. (B) Langmuir isotherms measured during compression of monolayers of amphiphile $\mathbf{1}_{10}$ (black) or Lipid A (gray) at air/water interfaces at 25 °C.

formation of a monolayer at the aqueous/LC interface. These results support our conclusion that the structure of this six-tailed amphiphile allows it to drive ordering transitions in LC droplets through a novel mechanism that is similar to that of Lipid A (see additional discussion below).

Past studies of ordering transitions in LC droplets using endotoxin and Lipid A have led to the hypothesis that these natural six-tailed amphiphiles promote changes in the configurations of LC droplets (from bipolar to radial) through a mechanism involving the formation of inverted self-associated lipid nanostructures at topological defects in the LC droplets (Figure 1D, red arrows; these defects correspond to regions of high strain where LC order is reduced).[9,18] This mechanism differs substantially from that involving one- and two-tailed surfactants (described above). The tendency of an amphiphile to adopt inverted self-assembled nanostructures is dependent, in part, on the ratio of headgroup area to molecular volume (the so-called "packing parameter").[22,28] Because amphiphile $\mathbf{1}_{10}$ has the same number and approximate tail length as Lipid A, the molecular volumes of the two should be similar. To determine if amphiphile $\mathbf{1}_{10}$ possesses a molecular area comparable to Lipid A, and thus a comparable packing parameter, we characterized their interfacial molecular areas by measuring Langmuir isotherms at air/water interfaces. A comparison of the isotherms of these two species (Figure 2B) reveals the mean molecular area of $\mathbf{1}_{10}$ and Lipid A to be ~175 and ~150 Å^2, respectively, suggesting that like Lipid A, amphiphile $\mathbf{1}_{10}$ can assume a packing geometry consistent with formation of inverted self-associated nanostructures. We note here, however, that there are also some significant differences between the two isotherms in Figure 2B, including evidence of phase transitions at intermediate surface pressures for Lipid A that are not apparent for amphiphile $\mathbf{1}_{10}$.

DOI: 10.1021/acs.langmuir.5b03557
Langmuir 2015, 31, 12850−12855

To explore other potential similarities in the fundamental self-assembly behaviors of amphiphile $\mathbf{1}_{10}$ and Lipid A that could provide insight into the results described above, we used small-angle X-ray scattering (SAXS) to characterize the nanostructures formed by these amphiphiles in bulk solution (i.e., in water or aqueous buffer, and not in the presence of LC droplets). Pure amphiphile $\mathbf{1}_{10}$ did not form lyotropic liquid crystalline phases in water or in phosphate-buffered saline that we could observe by SAXS. We note, however, that Lipid A possesses negatively charged phosphate functionality in its headgroup (Figure 1A) that is expected to influence self-assembly. Acidification of solutions of amphiphile $\mathbf{1}_{10}$ (0.133 wt % in 1.0 M aqueous H_2SO_4) to protonate the amines in the headgroup and promote formation of a multitailed, cationic analogue of Lipid A led to the immediate precipitation of lyotropic liquid crystalline particles. SAXS profiles for amphiphile $\mathbf{1}_{10}$ exhibited an unusual peak pattern under these conditions, including four high intensity peaks located at $q^*\sqrt{3}$, $q^*\sqrt{4}$, $q^*\sqrt{5}$, and $q^*\sqrt{6}$ (where $q^* = 0.1258$ Å^{-1}) (Figure 3).

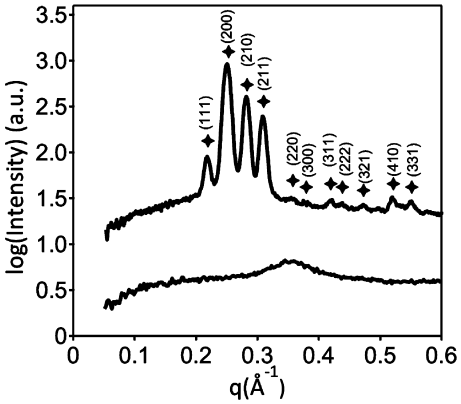

Figure 3. SAXS patterns for amphiphile $\mathbf{1}_{10}$ (upper) and amphiphile $\mathbf{1}_6$ (lower) in 1 M aqueous H_2SO_4 at 22 °C. Peak markers correspond to positions of expected reflections for a cubic morphology with $P4_232$ symmetry with unit cell dimension $d = 50$ Å ($q^* = 0.126$ Å^{-1}).

These scattering maxima are tentatively ascribed to the (111), (200), (210), and (211) reflections of a micellar cubic phase with $P4_232$ symmetry (space group #208) with a unit cell dimension $d = 50$ Å. The persistence of this lyotropic phase in the presence of excess acid solution strongly suggests that amphiphile $\mathbf{1}_{10}$ forms an inverse phase. This result is similar in some important ways to the previously reported lyotropic liquid crystalline phase behavior of Lipid A, which also forms inverse cubic phases at high water content.[21,22,29,30] We note in this context that past SAXS studies have investigated the bulk solution phase behaviors of Lipid A using conditions different from the strongly acidic conditions used here,[21,22] and that more explicit comparisons between the self-assembly behaviors of Lipid A and amphiphile $\mathbf{1}_{10}$ should thus be made with caution. Nevertheless, the results shown in Figure 3 demonstrate that amphiphile $\mathbf{1}_{10}$ can form inverse phases in aqueous solution, and provide support for the proposition that amphiphile $\mathbf{1}_{10}$, like Lipid A, can trigger transitions of LC droplets at ultralow concentrations via the formation of inverted nanostructures at defects in the LC droplets.

Experiments performed using amphiphiles $\mathbf{1}_6$, $\mathbf{1}_8$, $\mathbf{1}_{12}$, and $\mathbf{1}_{16}$ revealed the impact of tail length on the interfacial behavior of this class of six-tailed amphiphiles at aqueous/LC interfaces. As shown in Figure 4A, amphiphiles $\mathbf{1}_8$ and $\mathbf{1}_{12}$, possessing

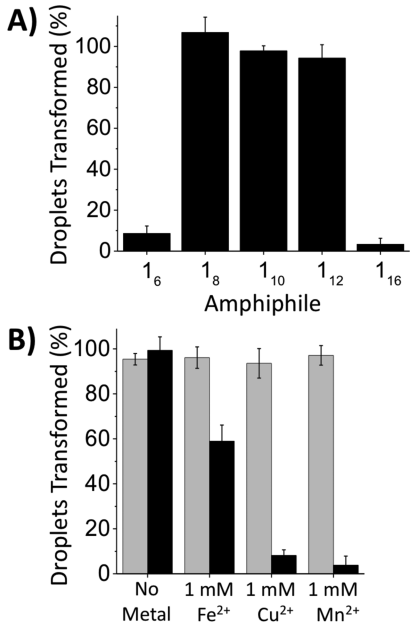

Figure 4. (A) Percentage of LC droplets transformed as a function of amphiphile tail length using amphiphiles $\mathbf{1}_6$–$\mathbf{1}_{16}$ ([1] = 500 pg/mL). (B) Percentage of LC droplets transformed in solutions of amphiphile $\mathbf{1}_{10}$ (black) or Lipid A (gray) in the presence or absence of $FeSO_4$, $CuSO_4$, or $MnCl_2$ ($[M^{2+}] = 1$ mM, $[\mathbf{1}_{10}] = 500$ pg/mL).

aliphatic tails 8 and 12 carbons in length, were also able to trigger LC droplets (at concentrations of 500 pg/mL). In contrast, species with tails 6 or 16 carbons in length ($\mathbf{1}_6$ and $\mathbf{1}_{16}$) did not. The apparent insensitivity of LC droplets to the presence of amphiphile $\mathbf{1}_{16}$ is likely a result of the sparing water solubility of this amphiphile under the conditions used here. We speculate that the inability of amphiphile $\mathbf{1}_6$ to trigger ordering transitions in LC droplets arises from the influence of its shorter tail length on self-assembly. Langmuir isotherms revealed molecular areas at air/water interfaces to decrease significantly with decreasing tail length (from ∼175 Å^2 for amphiphile $\mathbf{1}_{10}$ to ∼105 Å^2 for amphiphile $\mathbf{1}_6$; see Figure S2). In addition, SAXS characterization of amphiphile $\mathbf{1}_6$ in 1.0 M H_2SO_4 indicates that it does not self-assemble into the inverse cubic lyotropic phase observed with amphiphile $\mathbf{1}_{10}$ (Figure 3) under the conditions investigated here. Our results suggest that a critical amphiphile tail length is required to drive self-assembly into nanostructures that trigger ordering transitions in LC droplets.

Amphiphiles $\mathbf{1}_8$, $\mathbf{1}_{10}$, and $\mathbf{1}_{12}$ mimic the ability of Lipid A to trigger ordering transitions in LC droplets at exceedingly low concentrations. We note, however, that these amphiphiles have a headgroup functionality that differs substantially from the disaccharide-based headgroup of Lipid A, and that could endow these synthetic structures with the potential to respond to environmental stimuli in ways that Lipid A does not (e.g., to changes in pH or the chelation of multivalent metal ions, etc.). To explore the potential utility of this new structural feature, we performed a final series of proof-of-concept experiments to determine whether the ability of amphiphile $\mathbf{1}_{10}$ to trigger configurational transitions in LC droplets could be modulated by the presence of divalent metal ions in the aqueous phase (using flow cytometry to quantify changes in droplet configurations, as described above). As shown in Figure 4B (gray bars), the responses of LC droplets to Lipid A remained

DOI: 10.1021/acs.langmuir.5b03557
Langmuir 2015, 31, 12850−12855

insensitive to the addition of three divalent metal ions (Fe^{2+}, Cu^{2+}, Mn^{2+}; [M^{2+}] = 1 mM, [$\mathbf{1}_{10}$] = 500 pg/mL; pH = 7.2) under these conditions. However, as shown in Figure 4B (black bars), the responses of LC droplets to amphiphile $\mathbf{1}_{10}$ were strongly suppressed (to extents that varied with the identity of the metal ion used). This stimuli-responsive behavior is consistent with chelation of the metal ions by the polyamine headgroup of $\mathbf{1}_{10}$ and subsequent associated changes in self-assembly. Additional studies will be necessary to characterize the sensitivity of these six-tailed amphiphiles to the presence of ions and understand their impacts on self-assembly and the apparent selectivity (e.g., Fe^{2+} relative to Cu^{2+} or Mn^{2+}) shown in Figure 4B. The results of these initial experiments, however, suggest potential opportunities to use amphiphile $\mathbf{1}_{10}$ in combination with LC droplets to report the presence of specific ions in aqueous environments. More broadly, the nature of the polyamine headgroup in these synthetic amphiphiles could also enable the design of amphiphile/LC droplet systems that respond to changes in a broader range of environmental stimuli (pH, ionic strength, etc.).

SUMMARY AND CONCLUSIONS

In summary, the synthetic amphiphiles reported here mimic key features of the structure, interfacial behaviors, and self-assembly of Lipid A and provide insight into the origins of the ultrasensitive response of LC droplets to Lipid A. We anticipate that the materials and guiding principles reported here will enable the design of colloidal LC droplet systems that respond with exquisite sensitivity to chemical and biological stimuli and open the door to new applications of this emerging class of responsive soft matter.

ASSOCIATED CONTENT

Supporting Information

The Supporting Information is available free of charge on the ACS Publications website at DOI: 10.1021/acs.langmuir.5b03557.

Detailed description of experimental procedures and characterization of synthetic amphiphiles (PDF)

AUTHOR INFORMATION

Corresponding Authors

*E-mail: maheshkm@umn.edu.
*E-mail: nlabbott@wisc.edu.
*E-mail: david.lynn@wisc.edu.

Present Address

[‖]M.K.M.: Department of Chemical Engineering and Materials Science, 421 Washington Ave. SE, University of Minnesota, Minneapolis, MN 55455.

Author Contributions

[§]M.C.D.C. and D.S.M. contributed equally.

Notes

The authors declare the following competing financial interest(s): N.L.A. declares a financial interest in Platypus Technologies, LLC.

ACKNOWLEDGMENTS

This work was supported by the NSF (DMR-1121288, CHE-9974839, CHE-1048642), the ARO (W911NF-11-1-0251 and W911NF-14-1-0140), and the NIH (AI092004), and made use of facilities supported through NSF (MRSEC, DMR-1121288). M.C.D.C acknowledges the Natural Sciences and Engineering Research Council of Canada for a graduate fellowship.

REFERENCES

(1) Badjic, J. D.; Nelson, A.; Cantrill, S. J.; Turnbull, W. B.; Stoddart, J. F. Multivalency and cooperativity in supramolecular chemistry. *Acc. Chem. Res.* **2005**, *38*, 723−732.

(2) Woltman, S. J.; Jay, G. D.; Crawford, G. P. Liquid-crystal materials find a new order in biomedical applications. *Nat. Mater.* **2007**, *6*, 929−938.

(3) Aida, T.; Meijer, E. W.; Stupp, S. I. Functional Supramolecular Polymers. *Science* **2012**, *335*, 813−817.

(4) Yan, X.; Wang, F.; Zheng, B.; Huang, F. Stimuli-responsive supramolecular polymeric materials. *Chem. Soc. Rev.* **2012**, *41*, 6042−6065.

(5) Zhuang, J.; Gordon, M. R.; Ventura, J.; Li, L.; Thayumanavan, S. Multi-stimuli responsive macromolecules and their assemblies. *Chem. Soc. Rev.* **2013**, *42*, 7421−7435.

(6) Brake, J. M.; Daschner, M. K.; Luk, Y. Y.; Abbott, N. L. Biomolecular interactions at phospholipid-decorated surfaces of liquid crystals. *Science* **2003**, *302*, 2094−2097.

(7) Price, A. D.; Schwartz, D. K. DNA Hybridization-Induced Reorientation of Liquid Crystal Anchoring at the Nematic Liquid Crystal/Aqueous Interface. *J. Am. Chem. Soc.* **2008**, *130*, 8188−8194.

(8) Gupta, J. K.; Sivakumar, S.; Caruso, F.; Abbott, N. L. Size-Dependent Ordering of Liquid Crystals Observed in Polymeric Capsules with Micrometer and Smaller Diameter. *Angew. Chem., Int. Ed.* **2009**, *48*, 1652−1655.

(9) Lin, I. H.; Miller, D. S.; Bertics, P. J.; Murphy, C. J.; de Pablo, J. J.; Abbott, N. L. Endotoxin-induced structural transformations in liquid crystalline droplets. *Science* **2011**, *332*, 1297−300.

(10) Alino, V. J.; Pang, J.; Yang, K. L. Liquid Crystal Droplets as a Hosting and Sensing Platform for Developing Immunoassays. *Langmuir* **2011**, *27*, 11784−11789.

(11) McUmber, A. C.; Noonan, P. S.; Schwartz, D. K. Surfactant-DNA interactions at the liquid crystal-aqueous interface. *Soft Matter* **2012**, *8*, 4335−4342.

(12) Alino, V. J.; Sim, P. H.; Choy, W. T.; Fraser, A.; Yang, K.-L. Detecting Proteins in Microfluidic Channels Decorated with Liquid Crystal Sensing Dots. *Langmuir* **2012**, *28*, 17571−17577.

(13) Bera, T.; Fang, J. Polyelectrolyte-coated liquid crystal droplets for detecting charged macromolecules. *J. Mater. Chem.* **2012**, *22*, 6807−6812.

(14) Kim, J.; Khan, M.; Park, S. Y. Glucose Sensor using Liquid-Crystal Droplets Made by Microfluidics. *ACS Appl. Mater. Interfaces* **2013**, *5*, 13135−13139.

(15) Noonan, P. S.; Roberts, R. H.; Schwartz, D. K. Liquid Crystal Reorientation Induced by Aptamer Conformational Changes. *J. Am. Chem. Soc.* **2013**, *135*, 5183−5189.

(16) Chang, C.-Y.; Chen, C.-H. Oligopeptide-decorated liquid crystal droplets for detecting proteases. *Chem. Commun.* **2014**, *50*, 12162−12165.

(17) Miller, D. S.; Wang, X.; Abbott, N. L. Design of Functional Materials Based on Liquid Crystalline Droplets. *Chem. Mater.* **2014**, *26*, 496−506.

(18) Miller, D. S.; Abbott, N. L. Influence of droplet size, pH and ionic strength on endotoxin-triggered ordering transitions in liquid crystalline droplets. *Soft Matter* **2013**, *9*, 374−382.

(19) Molinaro, A.; Holst, O.; Di Lorenzo, F.; Callaghan, M.; Nurisso, A.; D'Errico, G.; Zamyatina, A.; Peri, F.; Berisio, R.; Jerala, R.; Jimenez-Barbero, J.; Silipo, A.; Martin-Santamaria, S. Chemistry of Lipid A: At the Heart of Innate Immunity. *Chem. - Eur. J.* **2015**, *21*, 500−519.

(20) Matsuura, M. Structural modifications of bacterial lipopolysaccharide that facilitate Gram-negative bacteria evasion of host innate immunity. *Front. Immunol.* **2013**, *4*, 1−9.

(21) Brandenburg, K.; Koch, M. H. J.; Seydel, U. Phase-Diagram of Lipid-A from *Samonella minnesota* and *Escherichia coli* Rough Mutant Lipopolysaccharide. *J. Struct. Biol.* **1990**, *105*, 11−21.

DOI: 10.1021/acs.langmuir.5b03557
Langmuir 2015, 31, 12850−12855

(22) Brandenburg, K.; Seydel, U.; Schromm, A. B.; Loppnow, H.; Koch, M. H. J.; Rietschel, E. T. Conformation of lipid A, the endotoxic center of bacterial lipopolysaccharide. *Innate Immun.* **1996**, *3*, 173−178.
(23) Love, K. T.; Mahon, K. P.; Levins, C. G.; Whitehead, K. A.; Querbes, W.; Dorkin, J. R.; Qin, J.; Cantley, W.; Qin, L. L.; Racie, T.; Frank-Kamenetsky, M.; Yip, K. N.; Alvarez, R.; Sah, D. W. Y.; de Fougerolles, A.; Fitzgerald, K.; Koteliansky, V.; Akinc, A.; Langer, R.; Anderson, D. G. Lipid-like materials for low-dose, *in vivo* gene silencing. *Proc. Natl. Acad. Sci. U. S. A.* **2010**, *107*, 1864−1869.
(24) Sun, S.; Wang, M.; Knupp, S. A.; Soto-Feliciano, Y.; Hu, X.; Kaplan, D. L.; Langer, R.; Anderson, D. G.; Xu, Q. B. Combinatorial Library of Lipidoids for *in vitro* DNA Delivery. *Bioconjugate Chem.* **2012**, *23*, 135−140.
(25) Zhang, Y. L.; Pelet, J. M.; Heller, D. A.; Dong, Y. Z.; Chen, D. L.; Gu, Z.; Joseph, B. J.; Wallas, J.; Anderson, D. G. Lipid-Modified Aminoglycoside Derivatives for *in vivo* siRNA Delivery. *Adv. Mater.* **2013**, *25*, 4641−4645.
(26) Sun, S.; Wang, M.; Alberti, K. A.; Choy, A.; Xu, Q. B. DOPE facilitates quaternized lipidoids (QLDs) for *in vitro* DNA delivery. *Nanomedicine* **2013**, *9*, 849−854.
(27) Miller, D. S.; Wang, X.; Buchen, J.; Lavrentovich, O. D.; Abbott, N. L. Analysis of the Internal Configurations of Droplets of Liquid Crystal Using Flow Cytometry. *Anal. Chem.* **2013**, *85*, 10296−10303.
(28) Israelachvili, J. N. *Intermolecular and Surface Forces*, revised 3rd ed.; Academic Press, New York, 2011.
(29) Seydel, U.; Brandenburg, K.; Koch, M. H. J.; Rietschel, E. T. Supramolecular Structure of Lipopolysaccharide and Free Lipid A under Physiological Conditions as Determined by Synchrotron Small-Angle X-Ray-Diffraction. *Eur. J. Biochem.* **1989**, *186*, 325−332.
(30) Brandenburg, K.; Koch, M. H. J.; Seydel, U. Phase-Diagram of Deep Rough Mutant Lipopolysaccharide from *Salmonella minnesota* R595. *J. Struct. Biol.* **1992**, *108*, 93−106.

DOI: 10.1021/acs.langmuir.5b03557
Langmuir 2015, 31, 12850−12855